Supporting Information for "AI Facilitated Fluoro-Electrochemical Phytoplankton Classification"

Haotian Chen, [a],[†] Samuel Barton,[b],[†], Minjun Yang,[a] Rosalind E.M.Rickaby,[b] Heather A. Bouman[b] and Richard G. Compton*[a]

[a] Physical and Theoretical Chemistry Laboratory, Department of Chemistry, University of Oxford, South Parks Road, Oxford OX1 3QZ, Great Britain

[b] Department of Earth Sciences, University of Oxford, South Parks Road, Oxford OX1 3AN, UK

[†] These authors contributed equally to this work.

* Corresponding author: richard.compton@chem.ox.ac.uk

Table of Contents

1 Experimental Procedures

1.1 Phytoplankton Samples

Data on a total of 29 strains of phytoplankton were collected, comprising 3325 images and 2911 fluorescence transients. Table S1 summarizes the species names, taxonomic orders, groups of ecological/biogeochemical relevance, and other information for the dataset. Figure S1 shows two pie

charts showing the distribution dataset by ecological groups. The dataset is very balanced and is a good proxy of real-world phytoplankton classification challenge.

Table S1. A summary of the phytoplankton culture and images or transient data collected from the culture.

ID	Name	Order	Ecologicalgrouping	# Images	# Transients	Phytoplankton Culture Sources
1	*Phaeodactylum tricornutum*	*Bacillariophyta*	Diatom	122	97	Roscoff Culture Collection (RCC69)
2	*Skeletonema japonicum*	*Thalassiosirales*	Diatom	75	71	Roscoff Culture Collection (RCC74)
3	*Thalassiosira weissflogii*	*Thalassiosirales*	Diatom	52	51	Roscoff Culture Collection (RCC76)
4	*Nitzchia* sp.	*Bacillariophyta*	Diatom	82	79	Roscoff Culture Collection (RCC80)
5	*Nitzchia closterium*	*Bacillariophyta*	Diatom	73	63	Roscoff Culture Collection (RCC81)
6	*Chrysotila dentata*(1)	*Coccolithales*	Coccolithophores	71	69	Marine Biological Association (PLY378)
7	*Chrysotila dentata*(2)	*Coccolithales*	Coccolithophores	114	107	Marine Biological Association (PLY406)
8	*Emiliania huxleyi* (morphotype A, light tomoderately calcified)	*Isochrysidales*	Calcifying Isochrysidales	225	205	Roscoff Culture Collection (RCC911)
9	*Thalassiosira pseudonana*	*Thalassiosirales*	Diatom	104	60	Roscoff Culture Collection (RCC950)
10	*Halamphora coffeaeformis*	*Naviculales*	Diatom	61	39	Culture Collection of Algae and

						Protozoa (CCAP1001/2)
11	*Calcidiscus leptoporus* (1)	*Coccolithales*	Coccolithophores	134	119	Roscoff Culture Collection (RCC1130)
12	*Calcidiscus leptoporus* (2)	*Coccolithales*	Coccolithophores	68	59	Roscoff Culture Collection (RCC1150)
13	*Calyptrosphaera sphaeroidea*	*Coccolithales*	Coccolithophores	119	93	Roscoff Culture Collection (RCC1178)
14	*Coccolithus braarudii*	*Coccolithales*	Coccolithophores	55	52	Roscoff Culture Collection (RCC1198)
15	*Emiliania huxleyi* (morphotype A/R, overercalcified calcified shield components)	*Isochrysidales*	Calcifying Isochrysidales	284	278	Roscoff Culture Collection (RCC1216)
16	*Emiliania huxleyi* (haploid version of RCC1216)	*Isochrysidales*	Calcifying Isochrysidales	142	117	Roscoff Culture Collection (RCC1217)
17	*Emiliania huxleyi* (naked/diploid version of RCC1731)	*Isochrysidales*	Calcifying Isochrysidales	100	84	Roscoff Culture Collection (RCC1242)
18	*Gephyrocapsa oceanica*	*Isochrysidales*	Calcifying Isochrysidales	138	132	Roscoff Culture Collection (RCC1314)
19	*Lepidodinium chlorophorum*	*Gymnodiniales*	Dinoflagellates	41	34	Roscoff Culture Collection (RCC1489)
20	*Thoracosphaera heimii*	*Thoracosphaerales*	Dinoflagellates	171	138	Roscoff Culture Collection (RCC1511)
21	*Emiliania huxleyi* (morphotype A, moderately calcified)	*Isochrysidales*	Calcifying Isochrysidales	328	322	Roscoff Culture Collection (RCC1731)
22	*Scyphosphaera apsteinii*	*Zygodiscales*	Coccolithophores	71	68	Roscoff Culture

						Collection (RCC3598)
23	*Coccolithus pelagicus*	*Coccolithales*	Coccolithophores	49	40	Roscoff Culture Collection (RCC3776)
24	*Coscinodiscus* sp.	*Coscinodiscales*	Diatom	48	40	Roscoff Culture Collection (RCC4273)
25	*Minidiscus variabilis*	*Thalassiosirales*	Diatom	179	126	Roscoff Culture Collection (RCC4657)
26	*Minidiscus comicus*	*Thalassiosirales*	Diatom	111	95	Roscoff Culture Collection (RCC4660)
27	*Scripsiella trochoidea*	*Thoracosphaerales*	Dinoflagellates	58	51	Marine Biological Association (PLY632)
28	*Heterocapsa triquetra*	*Peridiniales*	Dinoflagellates	74	62	Marine Biological Association (PLY717)
29	*Emiliania huxleyi* (morphotype A/R, overcalcified and_bulky_central region)	*Isochrysidales*	Calcifying Isochrysidales	176	160	Marine Biological Association (PLY853)

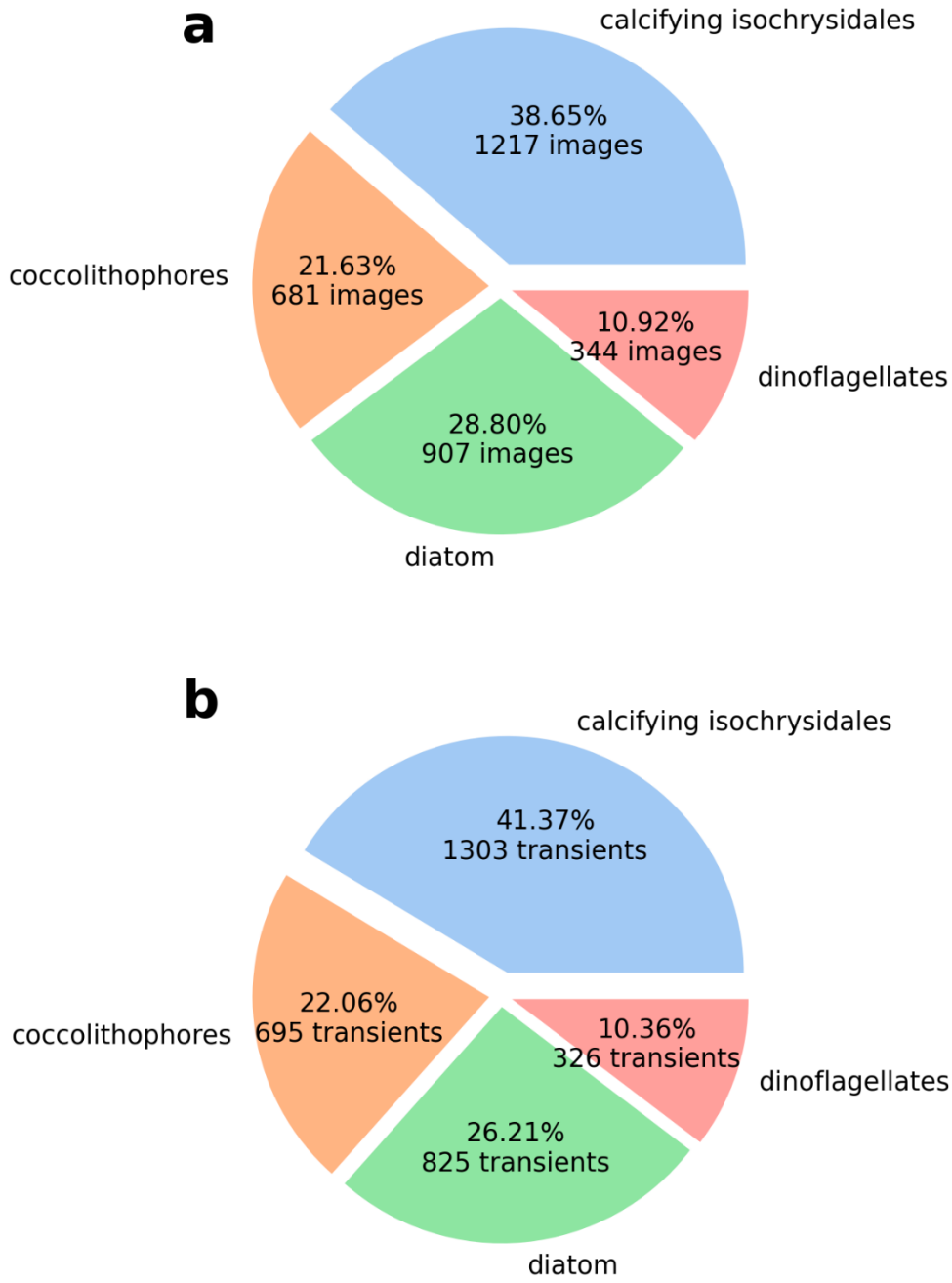

Figure S1. A pie chart illustrating the distribution of images(a) and fluorescence transients(b) samples by ecological groups.

1.2 Microscopy and Image Analysis

The optical images were taken on a Zeiss Axio Examiner, A1 Epifluorecence microscope (Carl Zeiss Ltd., Cambridge U.K.) using a 20× air objective (NA = 0.5, EC Plan-Neofluar). The excitation filter was supplied by Thorlab and the dichromic mirror and emission filter were a Zeiss filter set 15, transmitting emission wavelength above 590 nm. The excitation light source was a LQ-HXP 120V Lamp. The images and videos to extract fluorescence transients were recorded using a Hamamatsu ORCA-Flash 4.0 digital CMOS camera (Hamamatsu, Japan), providing 16-bit images with 4 MP resolution. The image was analyzed using ImageJ to locate phytoplankton. The intensity was extracted using a Zen 2 Pro. The effective area (A) of phytoplankton cells was analysed using ImageJ freeware (Fiji distribution)

threshold method so that the effective radius is calculated using the area of a circle equation ($A = \pi r^2$).

The imaging data for phytoplankton was processed using OpenCV and then resized to 80 pixels with equal width and height for deep learning datasets. No data transformation or data augmentation was performed.

1.3 Fluorescence transients

Measurement of fluorescence transients used a combination of the microscopy mentioned above and a 3D printed opto-electrochemical cell described elsewhere.[1] Briefly, an opto-electrochemical cell housed a three-electrode setup: a glassy carbon electrode (diameter = 3.00 mm, BASi, USA) as the working electrode, a saturated calomel electrode (SCE, ALS distributed by BASi, Tokyo, Japan) as the reference electrode and a graphite carbon rod as the counter electrode. Before the fuoro-electrochemical experiment, 50 µL of phytoplankton culture were dropcasted onto the electrode. The phytoplankton cells were allowed to settle onto the working electrode for approximately one minute before the cell was filled with electrolyte.

In the fluoro-electrochemical experiment the phytoplankton cells were first exposed to continuous fluorescence excitation (λ_{ex} = 475 ± 35nm) for 40 seconds. A series of fluorescence images were taken at 10 frames per second throughput the experiment. From t = 40s ($t = t_{on}$), a current was applied and ramped from 0 µA at a rate of 10 µA s^{-1} until the fluorescence from the cells was completely switched off.[1-2] The fluorescence transients were produced by integrating the intensity of a phytoplankton particle, and the intensity was normalized to unity using the value at t_{on}. Since the fluorescence images were taken 10 frames per second and the neural network used 19 seconds of transients, the transient data was transformed to the shape (190,1), where the former number represented the 190 data points and the latter number represented the single fluorescence channel.

2 Computational Methods

2.1 Neural networks facilitated phytoplankton classification

The two neural networks applied for either image recognition or fluorescence transient analysis were built using TensorFlow 2.3 and Keras in the Anaconda Python 3.7 environment.

2.1.1 Classification using Phytoplankton imaging

ResNet50V2[3] was directly imported from TensorFlow Keras applications library with pretrained weights from “imagenet”. The output layers were GlobalAveragePooling2D with fully connected layers, containing either 10 neurons for classification into taxonomic orders or 4 neurons for classification into ecological groups. Transfer learning with ResNet50V2 had two stages: a shorter first stage of initial training at a normal learning rate (10^{-3}) while freezing all layers except for the output layer and a longer second stage, fine tuning all layers at a very small learning rate (10^{-5}). The loss function was categorical cross entropy (introduced later), and the optimizer was Adam.[4] The network was trained for 10 epochs in the first stage and 50 epochs for the fine tuning stage. Recall that 10% of the training dataset was used for validation, the training and validation history was plotted in Figure S3. The training history showed high training accuracy after ~30 epochs of training, and validation accuracy stumbled around 85%, suggesting that the model was overfitted. The relatively low validation accuracy suggested that even with state-of-the-art network, images alone may not provide the most useful information.

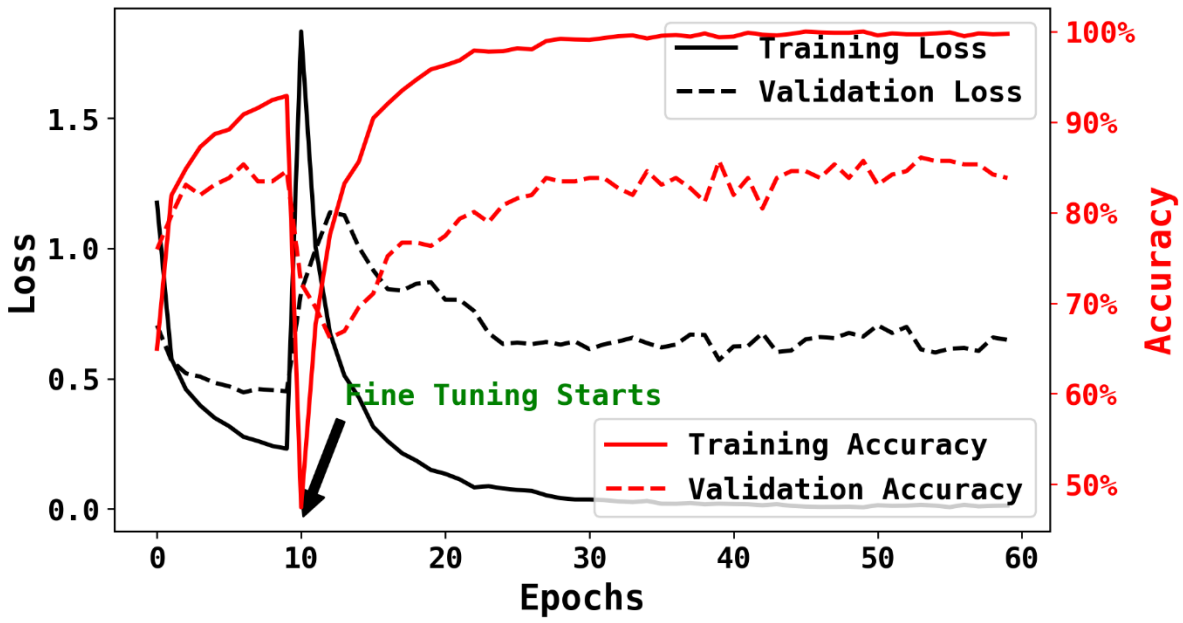

Figure S2. Training history of transfer learning using ResNet50V2. Initial training was before the 10th epoch and fine tuning was after the 10th epoch. The losses are shown on the left y-axis and the accuracy was shown on the right y-axis.

2.1.2 Classification using fluorescence transients

Classification of fluorescence transients used a home-made neural network specifically designed to adapt to the 1D fluorescence transient data. The network was called 1D Inception as two 1D inception blocks[5] were adopted in the network, providing strong discriminative power. Figure S3 illustrates the structure of the first inception block, containing three layers operating in parallel and detailed parameters allowing fully reproduction are shown in Table S2. After processing the input with two 1D inception blocks, the output was flattened and propagated through three fully-connected (dense) layers with decreasing width (800,400 and 100 neurons). The auxiliary input representing the radii of the phytoplankton was merged with the second hidden dense layer.

To classify transients into their taxonomic orders, the network was trained for 300 epochs. Figure S4 shows that training history as the 1D Inception neural network achieved a comparably high training and testing accuracy.

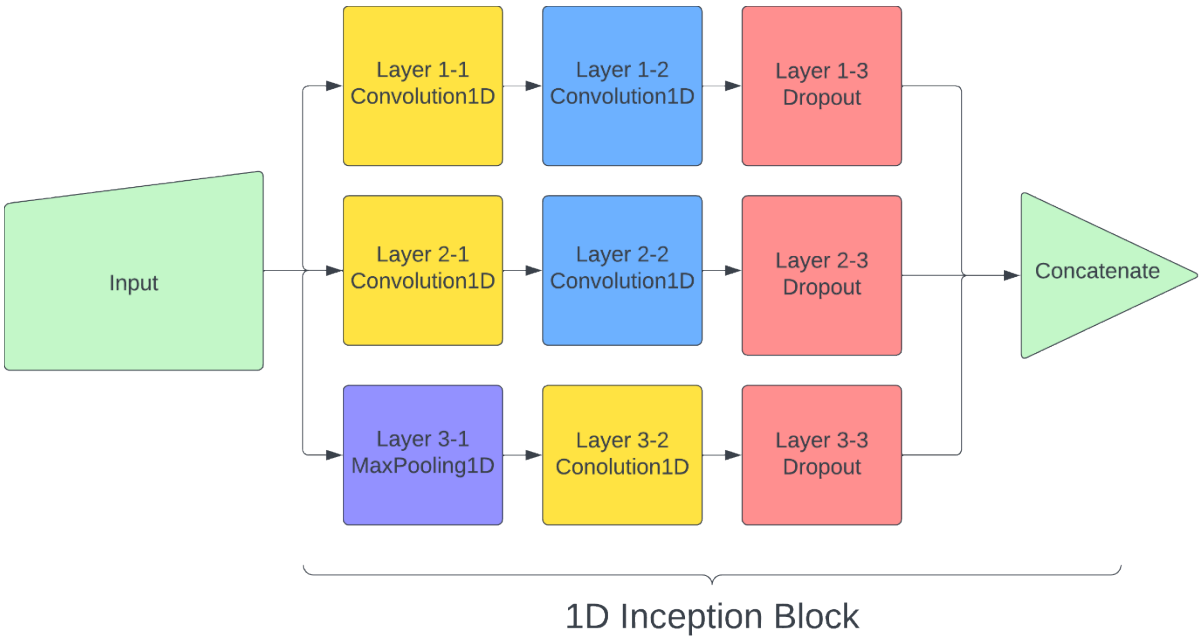

Figure S3. Schematic illustration of the structure of the 1D Inception block.

Table S2. Detailed parameters summary of 1D inception block.

Layer (type)	Output Size	Notes
Input (Input Layer)	(190,1)	-
Layer 1-1 (Convolution 1D)	(190,32)	Filters=32, kernel size=1, padding = 'same', activation = 'relu'.
Layer 1-2 (Convolution 1D)	(190,32)	Filters=32, kernel size=3, padding = 'same', activation = 'relu'.
Layer 1-3 (Dropout)	(190,32)	Dropout rate = 0.2
Layer 2-1 (Convolution 1D)	(190,32)	Filters=32, kernel size=1, padding = 'same', activation = 'relu'.
Layer 2-2 (Convolution 1D)	(190,32)	Filters=32, kernel size=5, padding = 'same', activation = 'relu'.
Layer 2-3 (Dropout)	(190,32)	Dropout rate = 0.2
Layer 3-1 (MaxPooling 1D)	(190,1)	Pool_size = 3, strides=1, padding = 'same'
Layer 3-2 (Convolution 1D)	(190,32)	Filters=32, kernel size=1, padding = 'same', activation = 'relu'.
Layer 3-3 (Dropout)	(190,32)	Dropout rate = 0.2
Concatenate (Concatenate)	(190,96)	Concatenates the outputs of Layer 1-3, Layer 2-3 and Layer 3-3.

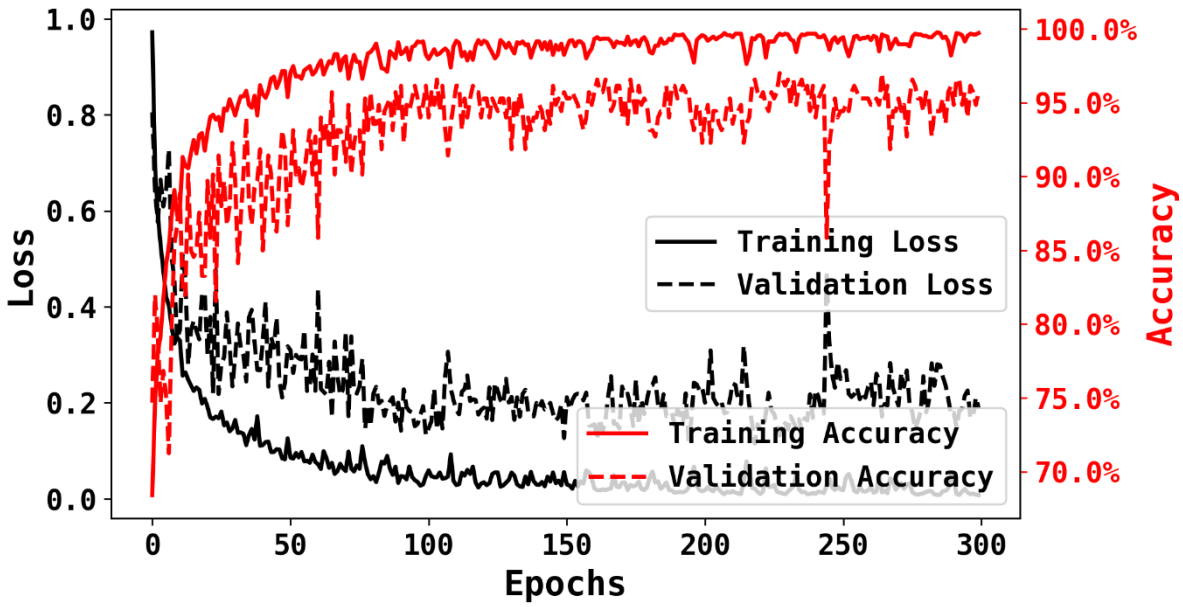

Figure S4. The training history of 1D Inception network on fluorescence transients with loss on the left y-axis and accuracy on the right y-axis.

2.1.3 Activation and loss functions for classifications

This section describes the activation and loss functions used for relevant neural network tasks.

The activation function for multiclass taxonomic classification was softmax:

$$\sigma(x)_i = \frac{e^{x_i}}{\sum_{j=1}^{K} e^{x_j}}$$

where σ is the softmax function, x_i are the inputs, and K is the total number of classes.

The activation function for binary identification was sigmoid:

$$\sigma(x) = \frac{1}{1 + e^{-x}}$$

The loss function for binary identification was binary cross entropy:

$$L = -(y \log p + (1 - y) \log (1 - p))$$

For a multiclass classification where $K > 2$, the loss function is categorical cross entropy:

$$L = -\sum_{i=1}^{K} y_{o,c} \log (p_{o,c})$$

where y is a binary indicator (0 or 1) if observation o can be correctly classified to class label c and p is the predicted probability observation o is of class c.

2.2 Phytoplankton classification using KNN and GridSearchCV

Phytoplankton could be classified to their taxonomic orders using just two parameters: half-lives and radii with the help K-Nearest Neighbour (KNN) method. The unit of half-life is second and unit of radii

is micrometre so that these two parameters are numerically comparable in scale. KNN algorithm classifies phytoplankton by finding and voting the taxonomic orders of its closest K neighbours, where K is a hyperparameter and the metric of "closest" neighbours is also to be defined. Thus, a GridSearchCV algorithm was applied to find the best hyperparameters for KNN algorithm to achieve the highest training accuracy. The search space is shown in Table S3. Note that the number of neighbours, K, are all odd numbers to prevent draws in voting. Using 5-fold cross validation of the training data, the optimal set of hyperparameters are found to be K=7, using Euclidean distance and uniform weighting. The training accuracy reached 89.0%. The testing accuracy reached 87.5%. The KNN and GridSearchCV methods were imported from Scikit-learn Python package.

Table S3.The hyperparameter search space for KNN classification.

Hyperparameter	Search Space
Number of neighbours, K	[3,5,7,9,11,13,15,17,19,21]
Distance metric	[Euclidean, Manhattan]
Weights	[uniform, distance]

3 References

[1] J. Yu, M. Yang, C. Batchelor-McAuley, S. Barton, R. E. M. Rickaby, H. A. Bouman, R. G. Compton, *ACS Measurement Science Au* **2022**, *2*, 342-350.

[2] M. Yang, C. Batchelor-McAuley, S. Barton, R. E. M. Rickaby, H. A. Bouman, R. G. Compton, *Environmental Science: Advances* **2022**, *1*, 156-163.

[3] K. He, X. Zhang, S. Ren, J. Sun, in *European conference on computer vision*, Springer, **2016**, pp. 630-645.

[4] D. P. Kingma, J. Ba, *arXiv preprint arXiv:1412.6980* **2014**.

[5] C. Szegedy, W. Liu, Y. Jia, P. Sermanet, S. Reed, D. Anguelov, D. Erhan, V. Vanhoucke, A. Rabinovich, in *Proceedings of the IEEE conference on computer vision and pattern recognition*, **2015**, pp. 1-9.